Available online at www.sciencedirect.com
SCIENCE DIRECT®
Scripta Materialia 51 (2004) 979–985
Scripta MATERIALIA
www.actamat-journals.com

Large reduction in critical stress in Co–Ni–Al upon repeated transformation

C. Efstathiou [a], H. Sehitoglu [a,*], A.J. Wagoner Johnson [a], R.F. Hamilton [a], H.J. Maier [b], Y. Chumlyakov [c]

[a] *Department of Mechanical and Industrial Engineering, University of Illinois, 1206 W. Green St., Urbana, IL 61801, USA*
[b] *University of Paderborn, Lehrstuhl f. Werkstoffkunde, D-33098 Paderborn, Germany*
[c] *Siberian Physical Technical Institute, Revolution Sq. 1, Tomsk 634050, Russia*

Received 25 June 2004; received in revised form 13 July 2004; accepted 20 July 2004
Available online 7 August 2004

Abstract

The stress–strain response of Co–Ni–Al with a two-phase microstructure displayed an unusual decrease in critical stress (84%) with strain or thermal cycling accompanied with an improved recoverability of pseudoelastic and shape memory strains. The pronounced decrease in critical stress occurred over a wide temperature range (145 °C), and is linked to the interaction of the transformation front with a secondary phase and the residual martensitic domains. The stabilized material is better suited for magnetic shape memory applications because of the lower elastic strain energy manifested through the lower critical stress and the reduced apparent elastic modulus. An extensive experimental program was utilized to establish the Clausius–Clapeyron relationship and the temperature dependence of critical stress for slip at elevated temperatures. A reduction of a factor of two in the slope of the Clausius–Clapeyron curve for the repeatedly deformed material was measured commensurate with the reduction in critical stress. The repeated deformation also produced a decrease in stress hysteresis and a reduction in residual strain making this material rather attractive for shape memory applications.

Keywords: Shape memory; Pseudoelasticity; Critical stress; Phase transformation; Ferromagnetic shape memory alloy; Hysteresis

1. Introduction

Newly developed transforming materials such as Co–Ni–Al exhibit a narrow thermal hysteresis (less than 30 °C), and ferromagnetic shape memory (FSM) behavior [1,2]. The ferromagnetic shape memory refers to motion of magnetic domains in the martensitic state under applied magnetic fields. The potential of this class of materials for actuation and sensing has generated considerable interest. However, their mechanical response is not fully understood. Recently, considerable focus has been devoted to FSM alloys such as Ni–Mn–Ga [3–5], which exhibit low ductility, as well as Fe–Pd [6,7] and Fe–Pt [8], which show smaller shape changes. The inherent brittleness and the high cost of constituent elements in all of these alloys make the Co–Ni–Al with its moderate ductility and lower cost an attractive alternative. Furthermore, it is well known that shape memory properties degrade with cycling in conventional shape memory alloys. The present work is undertaken to develop a better understanding of the cyclic response of Co–Ni–Al.

A range of compositions and heat treatments of Co–Ni–Al has been studied in the past in an effort to understand and develop precise phase diagrams [9–11]. A wide range of transformation and magnetic transition

* Corresponding author. Tel.: +1 217 333 4112; fax: +1 217 244 6534.
E-mail address: huseyin@uiuc.edu (H. Sehitoglu).

1359-6462/$ - see front matter © 2004 Acta Materialia Inc. Published by Elsevier Ltd. All rights reserved.
doi:10.1016/j.scriptamat.2004.07.014

temperatures can be tailored in these alloys by varying the Al content slightly [12,13]. Despite the increase in interest in Co–Ni–Al as a FSM alloy, its deformation response under repeated transformation and recovery has not been fully understood. This paper provides new information that addresses this need. Specifically, we present results compiled from nearly fifty experiments over a wide range of temperatures (−105 to 410 °C). We report for the first time the transient cyclic stress–strain response leading to stabilized behavior. A noteworthy difference between the present and the previous heat treatments was that the heat treatment was conducted at 1200 °C for 24 h resulting in a two-phase microstructure consisting of the β (ordered B2) and γ (ductile fcc) phases, rather than a single-phase microstructure more typical of other studies on Co–Ni–Al alloys.

The basis for shape memory behavior is the reversible thermoelastic martensitic transformation. Although the term thermoelastic implies completely reversible deformation, researchers have discovered irreversibilities following thermal and mechanical cycling [14,15]. Because these materials will be used in cyclic applications such as actuation, the degradation of recoverable deformation poses serious limitations. A number of investigations have shown a reduction in critical stress [16,17], a change in stress hysteresis [15,17,19], and an alteration of transformation temperatures [16] upon repeated transformation cycles in conventional shape memory alloys. The changes in critical stress have been confined to less than 30% in most cases. The underlying factor in these changes is the accumulated unrecovered (residual) strain during thermal and mechanical cycling and internal dissipation [15] producing large increases in hysteresis. Materials and conditions that circumvent these known trends require further study and elaboration, motivating a closer look at Co–Ni–Al alloys.

The purpose of this paper is to present data showing an unusually large decrease in critical stress resulting from cycling of up to 84%, which far exceeds previously reported levels in the literature for any shape memory materials. Our results demonstrate a critical stress–temperature relationship that is highly sensitive to the deformation history, but ultimately reaches stabilized stress levels. We explain this behavior using current understanding between internal stresses arising from defects and cyclic shape memory behavior.

2. Experimental procedure

The alloy investigated was cast to a nominal composition of Co–Ni34.5–Al28.3 (at.%). Transformation temperatures were determined using differential scanning calorimetry (DSC) for a range of heat treatments. Compression specimens (4 mm × 4 mm × 10 mm) were electrodischarge machined from the cast ingot, annealed at 1200 °C for 24 h, and water quenched. Compression tests were conducted using an Instron servohydraulic load frame and strain was measured with a miniature MTS extensometer (3 mm gauge length). Results in the temperature range of −105 to 100 °C were obtained via strain control while higher temperature tests were conducted using stroke control at strain rates of 10^{-4} s^{-1}. Following deformation, the specimens were heated to above the transformation temperature at zero load, which resulted in recovery of shape memory strains. A small unrecoverable strain remained at the conclusion of the heat-cool cycle and was monitored from cycle to cycle.

3. Results

Fig. 1(a) shows the β phase and the γ phase (secondary phase) present in the microstructure including the residual martensite. Fig. 1(b) is a micrograph at a higher magnification also showing both β and γ phases. These micrographs were obtained from deformed samples that were subsequently heated at zero load for the recovery of shape memory strains. We note that the transformation is confined to the β phase in both micrographs, and the martensite variant impinging on the secondary phase is visible in Fig. 1(b). The γ phase is known to improve the ductility of the otherwise brittle β phase [20]. Although the secondary phase does not undergo the

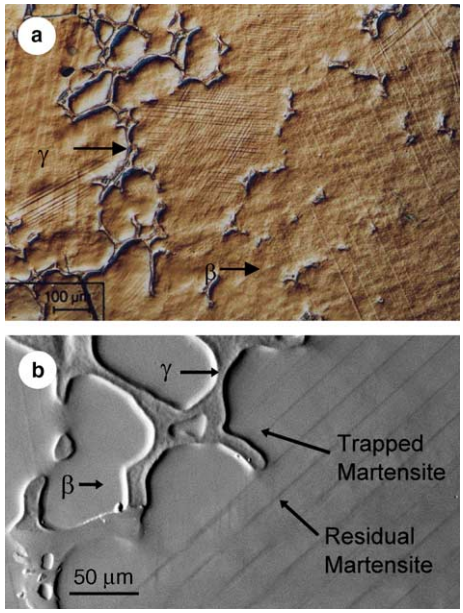

Fig. 1. Room temperature micrographs of Co–Ni34.5–Al28.3 heat treated at 1200 °C for 24 h: (a) lower magnification optical micrograph and (b) higher magnification scanning electron micrograph displaying the secondary phase and residual martensite. Note that the fine martensite variants are trapped by the secondary phase.

martensitic transformation, it influences the transformation due to interactions with moving martensite fronts. The results of the current study reflect the role of this interaction on the thermomechanical response of this alloy.

Transformation temperatures shown in Fig. 2 were determined from DSC peaks (as minimum and maximum points of the DCS curves), for annealing times ranging from 1 to 64 h. The as-cast material did not undergo the martensitic transformation in the temperature range −130 to 130 °C. The thermal hysteresis shown in Fig. 2 (the difference between the upper and lower curve) for the range of annealing times examined was measured to be approximately 22 °C. The 24 h annealing time was selected for mechanical testing because it displayed relatively high transformation temperatures, and because longer annealing times showed a negligible increase. The transformation temperatures for the 1200 °C–24 h heat treatment were −25 and −2 °C for the forward (A → M) and reverse (M → A) transformations, respectively.

Fig. 3 shows the stress–strain response for compression cycles at −22 and 100 °C. These loading temperatures were selected to represent two extreme cases of pseudoelasticity; the −22 °C loading temperature is near the A → M temperature, and the 100 °C loading temperature is near the M_d temperature, i.e. the temperature above which martensite can no longer be induced. The critical stress for each cycle is shown by the small arrows and was determined using an intersecting slopes method described as follows. A line was fit to the elastic portion of the curve and another line to the curve after the significant change in slope. The intersection of the two lines was considered the critical stress. Subsequent cycles showed a decrease in apparent modulus and therefore the procedure described was repeated for each sample and each cycle. Pseudoelastic recovery is defined as the

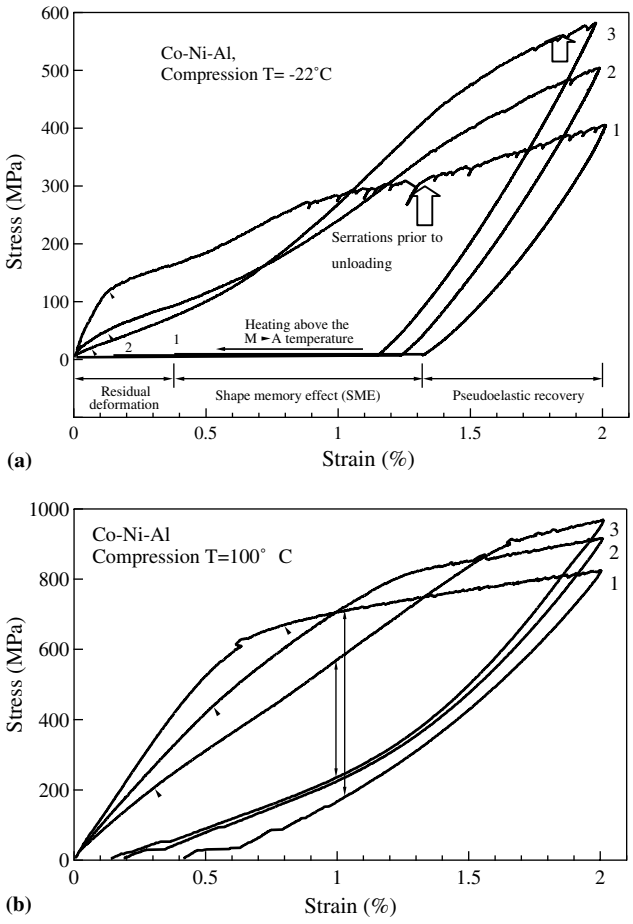

Fig. 3. Cyclic stress–strain results shown for two extreme temperatures demonstrating the improved recoverability of pseudoelastic and SME strains with cycling. By the third cycle the critical stress decreased in (a) by 98 MPa, or 84%, at −22 °C, and in (b) by 465 MPa, or 70%, at 100 °C. The small arrows indicate the critical stress at the onset of transformation. The large vertical arrows indicate the stress hysteresis. Stress drops (serrations) exist in the curves prior to unloading and are distinguished by large arrows in (a). The frequency of the serrations decreased with cycling.

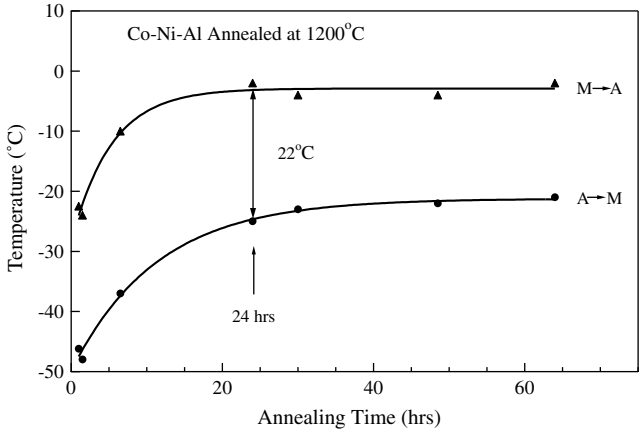

Fig. 2. Transformation temperatures for Co–Ni34.5–Al28.3 annealed at 1200 °C for different times. Thermal hysteresis was approximately 22 °C for all annealing times.

magnitude of recovered strain upon unloading. The strain caused by the shape memory effect (SME strain) is the recovered strain at zero stress during heating. These two strains are illustrated in Fig. 3(a). By the third cycle, in Fig. 3(a) and (b), the critical stress decreases by approximately 98 MPa, or 84%, at −22 °C and by 465 MPa, or 70%, at 100 °C, respectively. Notice the difference between the stress–strain response of the material during the first and the third cycles at both temperatures. The stress hysteresis also decreases with the increase in number of cycles, as is shown in Fig. 3(b) by the vertical arrows.

Common to both test temperatures, noticeable serrations (i.e. stress drops) exist in the first cycle stress–strain curves prior to unloading as indicate in Fig. 3(a). Serrations in the curve are more distinct at −22 °C as compared to 100 °C. These serrations could result from

the formation of different martensite variants within different grains or from the interaction of the transforming interface with the second phase constituent. It is apparent from Fig. 3 that cycling decreases the frequency of the serrations as well as their magnitude.

Stabilization of the stress–strain behavior was observed during cycling experiments. A sample was considered stabilized when the residual deformation saturates for a given applied strain upon cycling. Concomitant with stabilization, a distinct decrease in the frequency of stress drops prior to unloading is noticeable in Fig. 3. In Fig. 3(a), the first cycle showed 0.38% residual deformation, which progressively decreased in subsequent cycles until it became zero after the third cycle. Therefore, the sample was considered stabilized after the third cycle. In Fig. 3(b), the first cycle showed 0.42% residual deformation, and the third cycle showed a negligible change as compared to the second. Therefore, although residual deformation remained, the stress–strain response of the material was considered to be stable after the third cycle. A sample that showed only improved recoverability of pseudoelastic or SME strains was defined as moderately stabilized. An example of a moderately stabilized stress–strain response is shown by the second cycle in Fig. 3(a) and (b).

To illustrate this point further, Fig. 4 shows the stress–strain behavior of another stabilized specimen. The stabilization was introduced by thermally cycling the sample under small compressive stresses (<300 MPa) yielding 1.5% transformation strain while accumulating 0.3% residual deformation at 22 °C. The first and second cycles in Fig. 4 showed 100% recovery of the deformation after heating without serrations in the curves. Similar loading of a virgin sample did not generate as much recoverability as the stabilized sample and stress drops were observed. Although the third cycle recovered 100% of the deformation, serrations were observed prior to unloading indicating stabilization is only effective up to a strain limit, which for this case was 1.5%. Interestingly, this strain corresponds to the transformation strain achieved during the stabilization treatment. The fourth cycle introduced 0.16% unrecoverable deformation (shown by the arrow after heating) and the serrations disappeared signifying a secondary stabilization. Consequently, the fifth cycle represented the initial response of a specimen stabilized through thermal cycling under constant stress plus isothermal strain cycling. Compared to the fourth cycle, the critical stress decreased, the transformation exhibited a noticeable plateau stress over a larger strain range, and the SME was greatly enhanced for the fifth cycle. In this case, new martensite variants were activated as the strain was increased beyond the stabilization strain limit, and the critical stress was lowered in this case compared to the initial 'stabilized' value.

Another example of the stabilized stress–strain response is considered in Fig. 5 in which pseudoelastic behavior was observed. The specimen was subjected to five loading cycles in which the isothermal test temperature was increased for successive cycles. Only the third and the fifth cycles are shown, which were conducted at 40 and 100 °C, respectively. The first two loading cycles at room temperature resulted in 0.51% residual deformation. The third and fifth cycles recovered the total deformation (4%). For the pre-stabilized specimen the stress hysteresis decreased with increasing test temperature (comparing the 40 and 100 °C results). Compared to the virgin specimen in Fig. 3(b), the stabilization drastically improved the pseudoelastic recovery.

Fig. 6 illustrates the variation in critical stress with temperature for virgin, moderately stabilized, and stabilized material. As indicated in the figure, the slope of the

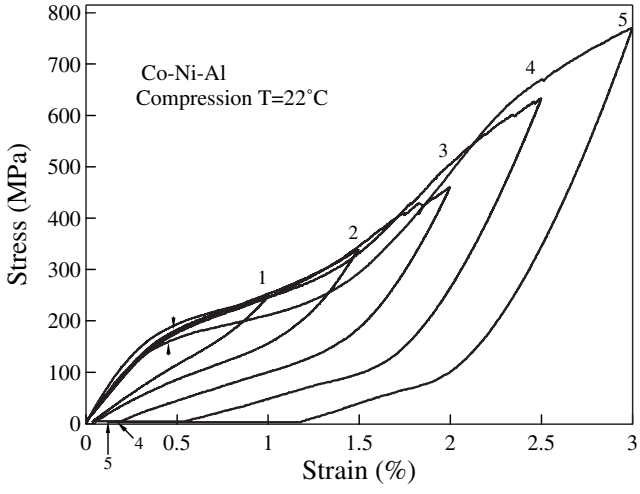

Fig. 4. Room temperature cyclic pseudoelastic stress–strain behavior of a pre-stabilized specimen.

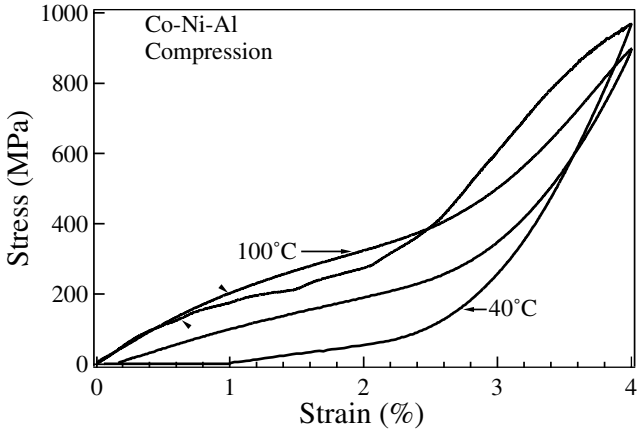

Fig. 5. The pseudoelastic response of a stabilized specimen at 40 °C (third cycle) and 100 °C (fifth cycle). The recoverable strain (including elastic recovery) is as high as 4% at 100 °C.

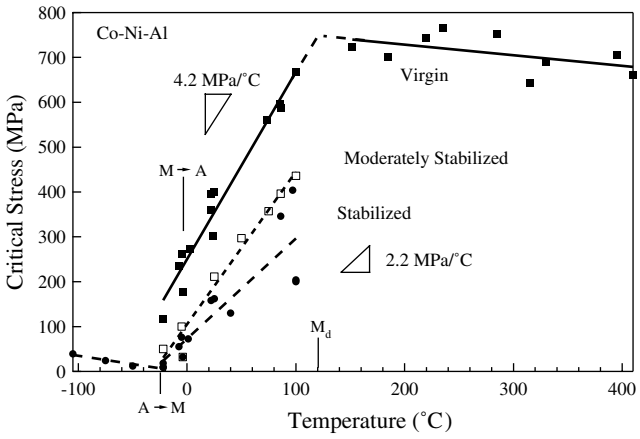

Fig. 6. Critical stress as a function of temperature showing the Clausius–Clapeyron relationship for the virgin material, moderately stabilized, and stabilized Co–Ni–Al.

curve was 4.2 and 2.2 MPa/°C for the virgin and stabilized materials, respectively. The temperature range over which stress-induced martensite formed was approximately 145 °C. This temperature regime is conventionally defined as the temperature range between the (A → M) transformation temperature and the M_d temperature and is significantly lower for the well known conventional shape memory alloys. Also noteworthy is the extremely low critical stress at test temperatures below the (A → M) transformation temperature for the stabilized material. The critical stresses observed at these temperatures are lower than those for NiTi and FeNiCoTi. Based on the results given in Fig. 6, no noticeable change occurred in A → M transformation temperature with repeated transformation cycles.

4. Discussion of results

The following key observations are noted and subsequently discussed for Co–Ni34.5–Al28.3 studied in this work. With an increase in the number of pseudoelastic cycles we found a significant decrease in critical stress; an improved recoverability of pseudoelastic and SME strains; a stabilization effect; a decrease in stress hysteresis, and an unusually large pseudoelastic window.

In previous studies the decrease in critical stress has been associated with the generation of dislocations and residual martensite after few transformation cycles [16,18,19,21]. These changes are typically less than 25% in NiTi and Cu-based shape memory alloys, and are therefore considerably smaller than the remarkable changes approaching 84% in this study. Dislocations readily form at transformation fronts depending on the slip resistance of these domains and the magnitude of the transformation shear strain. These dislocations prevent reverse transformation of a fraction of the martensite plates, which leads to the presence of residual martensite. The subsequent stress fields surrounding the residual martensite and the associated dislocation arrangements act to preferentially orient the nucleating variants of martensite to the externally applied stress, thus facilitating the subsequent transformation [21] from austenite to martensite. The residual martensite also acts as a new nucleation site [21]. Under pseudoelastic cycling, the development of these internal stress fields assists the driving force for the forward transformation, thereby contributing to the decreases in critical stress levels. It is evident, by the drastic decrease in critical stress shown in Fig. 3(a) and (b), that internal stress fields and enhanced nucleation sites have a more pronounced effect in Co–Ni–Al compared to other well known shape memory alloys. Finally, the secondary (ductile fcc) phase clearly provides an additional source of internal stresses, which is apparently unique to Co–Ni–Al with this heat treatment.

The secondary (ductile) phase in Co–Ni–Al does not undergo the transformation but could assist in trapping the martensite transformation fronts. Interaction between the secondary phase and the transformation front is evidenced by the serrations, including large stress drops, found during the first loading cycle in Fig. 3(a) between 0.7% and 2% strain. The abrupt stress drops and subsequent bursts in stress likely correspond to two phenomena: (i) the formation of different martensite variants (stress drops) when transforming martensite is trapped by the second phase or by dislocations, or (ii) local fluctuations in the thermodynamic driving force due to plastic relaxation of the transforming interface through dislocation emission as it bypasses the second phase. Residual martensite trapped by the γ phase was verified by optical and scanning electron microscopy (Fig. 1(a) and (b)). In the second cycle, defects (dislocations and residual martensite) resulting from phase boundary-second phase interaction during the first cycle produce internal stress fields that assist the forward transformation and therefore lower the critical stress. These contributions, coupled with the inherent cycling effects addressed earlier, produce the drastic decrease in critical stress after the first cycle. Defect generation eventually saturates with cycling leading to stabilization. Prior to saturation, the assistance from the internal stress fields is continually enhanced thus creating a more reversible transformation path for the subsequent cycles. The marked decrease in serrations after the first cycle (Fig. 3(a)) indicates that the secondary phase provides less resistance in subsequent cycles. Consequently, the decrease in critical stress from the second to the third cycle is significantly less than that from the first to the second. Therefore, after the first few passage of martensite front the critical stress approaches saturation or a 'stabilized' value. We also note that these stress drops are greatly reduced at temperatures near 85 °C

(at temperatures approaching the M_d temperature) and most prevalent near the A → M temperature.

The experimental results demonstrated that the recoverable strain increased with cycles reaching a 'stabilized' level. In successive cycles, we postulate that the density of dislocations and the volume fraction of residual martensite accrued during the transformation both decrease causing the reduction in residual strain. Residual strain remains if unrecoverable deformation resulting from the slip in austenite and martensite domains and the pre-existing residual martensite persists. The presence of preferential martensite nucleation and lowered resistance from the secondary γ phase reduces the plastic relaxation mechanisms thus lowering the residual strain. We postulate that stabilization leads to full recovery near the A → M transformation temperature, shown in Fig. 3(a), because deformation is mainly associated with the movement of twin boundaries, rearrangement of twin boundaries, and elastic deformation of martensite variants. We note that the residual deformation after stabilization at 100 °C (102 °C above the (A → M) transformation temperature), shown in Fig. 3(b), remains because slip occurs in austenite domains near the M_d temperature at such high stresses [22].

The stress hysteresis was examined as a function of temperature and pseudoelastic cycling. Fig. 3(b) shows a decrease in stress hysteresis with cycling (indicated with the vertical arrows). The stress hysteresis also decreases with cycling at an increased isothermal test temperature in Fig. 5. The decrease in hysteresis with transformation cycling results from decreased dissipation as discussed in a recent paper by Hamilton et al. [15]. Energy dissipation due to irreversible mechanisms such as frictional energy dissipation and stored elastic energy relaxation is responsible for the hysteresis size. Energy dissipation occurs: (i) when variants of martensite preferentially oriented to the applied stress interact with different variants oriented to internal stress fields, and (ii) when transforming variants interact with residual martensite or existing dislocations, and (iii) when plastic relaxation occurs at the phase boundaries. Multi-variant interactions and the resistance resulting from the interaction of the transforming interface with the γ phase are dissipative processes that dictate the stress hysteresis in pseudoelastic cycling. Since these contributions decrease with cycling, the hysteresis decreases. It has been reported that associated with repeated nucleation and growth of preferentially oriented martensite variants, dislocations rearrange so as to reduce frictional energy dissipation [19]. This lends further support to a decrease in stress hysteresis with transformation cycling.

In addition to the drastic decrease in critical stress, the increase in recoverability, and the decrease in stress hysteresis, we reported small critical stress levels below the A → M transformation temperature for the 'stabilized' material as compared to other shape memory alloys. The critical stress is approximately 10 MPa at the A → M transformation temperature. We note that the low critical stress is related to the frictional stress required for martensite rearrangement. The ability to induce magnetic field induced shape changes depends on a competition between magnetic energy and elastic strain energy. The reduction in both stress and apparent elastic modulus result in a lower elastic energy, which can be readily overcome by the magnetic energy. These features make this material an excellent candidate for ferromagnetic shape memory applications.

Finally, we emphasize that Co–Ni34.5–Al28.3 annealed at 1200 °C for 24 h produces a two-phase (β and γ) microstructure while a single-phase microstructure is obtained after annealing at 1350 °C or higher temperatures. The latter annealing schedule has been explored extensively in the literature, while the former treatment has not be investigated until the current study. Introducing the secondary phase, γ, is known to enhance ductility [20], but its effect on pseudoelastic cycling has not previously been examined until now. A smaller decrease in critical stress as a result of pseudoelastic cycling was previously reported in NiTi [16,18,19,23] and Cu-based shape memory alloys [21]. Miyazaki et al. [16] reported a decrease of approximately 15% after five cycles for samples deformed to 5% strain. Data from a study by Strnadel et al. [23] on Ti–Ni–Cu indicated a decrease of approximately 14% by the third cycle with samples deformed to 3% strain. The work of Karaca et al. [24] on Co–Ni–Al has investigated the first cycle response for a single-phase microstructure. The mechanisms for the substantial decrease in critical stress combined with the stress–temperature diagram and cyclic pseudoelastic effects demonstrate that the Co–Ni–Al system can be tailored to produce excellent shape memory and ferromagnetic shape memory characteristics. The results from this work also establish a large temperature range (145 °C) over which shape memory and pseudoelasticity can occur in these materials. This broad range of temperature increases the potential utility of these materials.

5. Conclusions

The following conclusions are drawn from this work:

- A significant decrease in critical stress as compared to other shape memory alloys was observed under repeated transformation cycling. The decrease was linked to modified internal stress fields associated with the residual martensite and dislocations, resulting from interaction between the transformation front and the secondary phase, which aid the forward

transformation in successive cycles. The low critical stress levels near the martensite start temperature sets the stage for ferromagnetic shape memory applications for this class of alloys.

- Repeated cycling produced preferential martensite variants and an internal stress pattern that continually decreases the unrecoverable deformation with cycling. Repeated transformations eventually saturate the residual strain, approaching a stabilized condition.
- The stress hysteresis decreased with increasing number of pseudoelastic cycles. The decrease was attributed to the reduced contribution from dissipation mechanisms associated with variant coalescence in the presence of internal stress fields. For varying annealing times, the narrow thermal hysteresis of approximately 22 °C remained constant despite the changing transformation temperatures, allowing this material to be used over a wide temperature range.
- The material exhibited a considerably larger pseudoelastic window of 145 °C as compared to traditional shape memory materials. Combined with the maximum pseudoelastic strains approaching 4% this alloy has potential benefits compared to other shape memory materials.

Acknowledgments

The work is supported partially by the AFOSR, Directorate of Aerospace and Materials Sciences and NSF grants CMS-0332824 and CMS-0428428. H.J. Maier acknowledges the support of Deutsche Forschungsgemeinschaft.

References

[1] Oikawa K, Wulff L, Lijima T, Gejima T, Ohmori T, Fujita A, et al. Appl. Phys. Lett. 2001;79:3290–2.
[2] Oikawa K, Omori T, Sutou Y. J Phys 2003;112:1017–20.
[3] Webster PJ, Ziebeck KRA, Towm SL, Pesk MS. Philos Mag 1985;49B:295.
[4] Vasil'ev AN, Kokorin VV, Savchenko YuI, Chernenko VA. Sov Phys JETP 1990;71:803.
[5] Chernenko VA, L'vov V, Pons J, Cesari E. J Appl Phys 2003;93:2394.
[6] James RD, Wuttig M. Philos Mag A 1998;77(5):1273–99.
[7] Muto S, Oshima R, Fujita FE. Scripta Mater 1987;465–468:21.
[8] Kakeshita T, Takeuchi T, Fukuda T, Tsujiguchi M, Saburi T, Oshima R. Appl Phys Lett 2000;77:1502–4.
[9] Kimura Y, Miura S, Suzuki T, Mishima Y. Mater Trans 1994;35:800–7.
[10] Kainuma R, Ise M, Jia CC, Ohatani H, Ishida K. Intermetallics 1996;4:S151–8.
[11] Oikawa K, Ota T, Gejima F, Ohmori T, Kainuma R, Ishida K. Mater Trans 2001;79:2472–5.
[12] Murakami Y, Shindo D, Oikawa K, Kainuma R, Ishida K. Acta Mater 2002;50:2173–84.
[13] Morito H, Fujita A, Fukamichi K, Kainuma R, Ishida K. Appl Phys Lett 2002;81:1657–9.
[14] Delaey L, Ortin J, Van Humbeeck J. Proc of Phase Transf 87. The Inst. of Metals; 1988. p. 60–6.
[15] Hamilton RF, Sehitoglu H, Chumlyakov H, Maier HJ. Acta Mater 2004;52:3383–402.
[16] Miyazaki S, Igo Y, Otsuka K. Acta Mater 1986;34:2045–51.
[17] Melton KN, Mercier O. Acta Mater 1979;27:137–44.
[18] Gall K, Sehitoglu H, Chumlyakov Y, Kireeva I. Scripta Mater 1999;40:7–12.
[19] McCormick PG, Liu Y. Acta Mater 1994;4:2407–13.
[20] Ishida K, Kainuma R, Ueno N, Nishizawa T. Metall Trans A 1991;22A:441–6.
[21] Perkins J, Muesing WE. Metall Trans A 1983;14A:33–6.
[22] Sehitoglu H, Karaman I, Anderson R, Zhang X, Gall K, Maier HJ, et al. Acta Mater. 2000;48:3311–26.
[23] Strnadel B, Ohashi S, Ohtsuka H, Ishihara T, Miyazaki S. Mater Sci Eng A 1995;A202:148–56.
[24] Karaca HE, Karaman I, Lagoudas DC, Maier HJ, Chumlyakov YI. Scripta Mater 2003;49:831–6.